Physics Letters A 376 (2012) 3530–3534

Contents lists available at SciVerse ScienceDirect

Physics Letters A

www.elsevier.com/locate/pla

Topological phases of the two-leg Kitaev ladder

Ning Wu

Department of Physics, Tsinghua University, Beijing 100084, China

ARTICLE INFO

Article history:
Received 30 June 2012
Accepted 10 October 2012
Available online 16 October 2012
Communicated by A.R. Bishop

Keywords:
Kitaev model
Topological transitions
Topological invariants

ABSTRACT

We study the phase diagram of the two-leg Kitaev model. Different topological phases can be characterized by either the number of Majorana modes for a deformed chain of the open ladder, or by a winding number related to the '*h*-loop' in the momentum space. By adding a three-spin interaction term to break the time-reversal symmetry, two originally different phases are glued together, so that the number of Majorana modes reduce to 0 or 1, namely, the topological invariant collapses to Z_2 from an integer Z. These observations are consistent with a recent general study [S. Tewari, J.D. Sau, arXiv:1111.6592v2].

1. Introduction

In a seminal work, Kitaev [1] showed that a Majorana bound state with zero energy can emerge at each end of a one-dimensional spinless p-wave superconductor. Different topological phases are distinguished by the presence or absence of such a mode, or a Z_2 topological invariant. Based on this, it was generally assumed that the time-reversal invariant topological superconductors are classified by a Z_2 invariant in one dimension [2–4]. However, motivated by an example study in Ref. [5], it is recently proposed [6] that a spin–orbit coupled topological semiconductor nanowire with time-reversal symmetry is indeed characterized by an integer Z topological invariant, which counts the number of Majorana zero modes at each end of the nanowire. The conventional Z_2 index only gives the parity of an integer invariant. Furthermore, the Z index reduces to Z_2 by external terms breaking the chirality symmetry. Here we give an alternative explicit example supporting these observations.

We study the topological phases of the two-leg Kitaev model [7]. It is found that distinct phases can be characterized by either the number of Majorana modes for a deformed chain of the open ladder, or by a winding number related to the '*h*-loop' in the momentum space. To break the time-reversal symmetry, we add a three-spin interaction term. This term opens a gap along one phase boundary, so that the originally two different phases separated by the phase boundary connect to each other to form a new phase. Correspondingly, the number of Majorana modes reduce to 0 or 1. In other words, the topological index collapses from Z to Z_2, which is consistent with Ref. [6].

E-mail address: wun1985@gmail.com.

0375-9601/$ – see front matter
http://dx.doi.org/10.1016/j.physleta.2012.10.016

2. The two-leg Kitaev ladder and Z invariants

The Kitaev model [7] on the honeycomb lattice is an exactly solvable model supporting topological orders. Recently, Feng, Zhang and Xiang [8] gave a beautiful different method of solution of the same model by transforming the spins into Jordan–Wigner fermions. They showed that the quantum phase transitions are of topological type and can be characterized by non-local string order parameters, which become local order parameters by proper dual transformations. These results indicate that different quantum phases can be classified by topological order parameters.

2.1. Mapping two-leg ladder spin model to free Majorana fermions

Consider the two-leg Kitaev open ladder with $2N$ spins-1/2 in each row (see Fig. 1(a)):

$$\begin{aligned} H = &\sum_{j=1}^{N}\left(J_1\sigma^x_{2j-1,1}\sigma^x_{2j,1} + J_2\sigma^y_{2j-1,2}\sigma^y_{2j,2}\right) \\ &+ \sum_{j=1}^{N-1}\left(J_2\sigma^y_{2j,1}\sigma^y_{2j+1,1} + J_1\sigma^x_{2j,2}\sigma^x_{2j+1,2}\right) \\ &+ J_3\sum_{j=1}^{N}\left(\sigma^z_{2j-1,1}\sigma^z_{2j-1,2} + \sigma^z_{2j,1}\sigma^z_{2j,2}\right), \end{aligned} \tag{1}$$

where $\sigma^{\mu}_{j,\alpha}$ are the Pauli matrices on the j-th site of row $\alpha = 1, 2$. By introducing the following Jordan–Wigner transformations $\frac{\sigma^x_{j,\alpha}+i\sigma^y_{j,\alpha}}{2} = a^{\dagger}_{j,\alpha}\prod_{i=1}^{j-1}(-\sigma^z_{i,\alpha})$, $\alpha = 1, 2$, and two sets of Majorana operators: $c_{j,\alpha} = -i(a_{j,\alpha} - a^{\dagger}_{j,\alpha})$, $d_{j,\alpha} = a_{j,\alpha} + a^{\dagger}_{j,\alpha}$, for

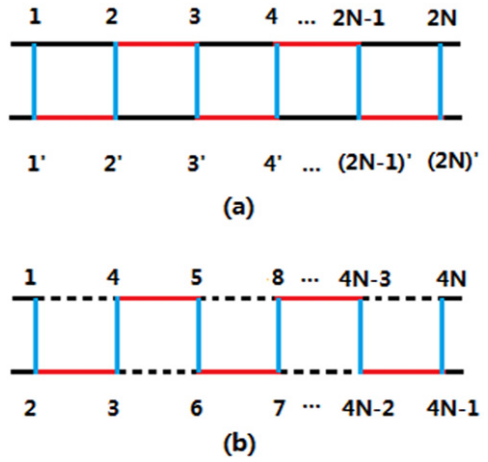

Fig. 1. (a) The two-leg Kitaev model. (b) A deformed snake-chain representation of the two-leg ladder.

$j+\alpha = even$; and $c_{j,\alpha} = a_{j,\alpha} + a^{\dagger}_{j,\alpha}$, $d_{j,\alpha} = -i(a_{j,\alpha} - a^{\dagger}_{j,\alpha})$, for $j+\alpha = odd$, the Hamiltonian is mapped onto a Majorana fermion model

$$\begin{aligned} H = &-i\sum_{j=1}^{N}(J_1 c_{2j-1,1}c_{2j,1} - J_2 c_{2j-1,2}c_{2j,2}) \\ &+ i\sum_{j=1}^{N-1}(J_2 c_{2j,1}c_{2j+1,1} - J_1 c_{2j,2}c_{2j+1,2}) \\ &+ iJ_3\sum_{j=1}^{N}(c_{2j-1,1}c_{2j-1,2}D_{2j-1} + c_{2j,1}c_{2j,2}D_{2j}), \end{aligned} \tag{2}$$

where $D_j \equiv id_{j,1}d_{j,2}$ is defined on each z-bond and is a good quantum number [8] and can be viewed as a classical Ising variable. We will set $J_1 > 0$ and $J_3 = 1$ henceforth.

The ground state of Eq. (2) should be in a π-flux phase from Lieb's theorem [9]. So the D's can be chosen as $D_{2j-1} = +1$, $D_{2j} = \mathrm{sgn}(J_2)$, depending on the sign of J_2. In the following we will focus on the case of $J_2 < 0$, where it is convenient to relabel the sites along a special path as shown in Fig. 1(b) to form a Majorana snake chain of $4N$ sites:

$$\begin{aligned} H_{snake} = &-i\sum_{j=1}^{2N} c_{2j-1}c_{2j} + iJ_2\sum_{j=1}^{2N-1} c_{2j}c_{2j+1} \\ &- iJ_1\sum_{j=1}^{2N-1} c_{2j-1}c_{2j+2}. \end{aligned} \tag{3}$$

2.2. Bulk properties

The snake chain is translationally invariant by two lattice spacings. In the thermodynamic limit $N \to \infty$, it can be diagonalized by the Fourier transformations $(c_{2j-1}, c_{2j})^T = \sqrt{\frac{1}{N}}\sum_k e^{ikj}\Psi_k$, $k \in [-\pi, \pi]$, where $\Psi_k = (a_k, b_k)^T$ satisfies $\Psi^{\dagger}_k = \Psi^T_{-k}$. Then

$$H_{snake} = \sum_k \Psi^{\dagger}_k[h_1(k)\sigma_1 + h_2(k)\sigma_2]\Psi_k, \tag{4}$$

where $h_1(k) = J_-\sin k$, $h_2(k) = 1 + J_+\cos k$, with $J_\pm = J_1 \pm J_2$. The spectra of excitations with particle–hole symmetry are given by $\pm|\mathbf{h}(k)|$,

$$\left|\mathbf{h}(k)\right| = \sqrt{J_-^2\sin^2 k + (1 + J_+\cos k)^2}. \tag{5}$$

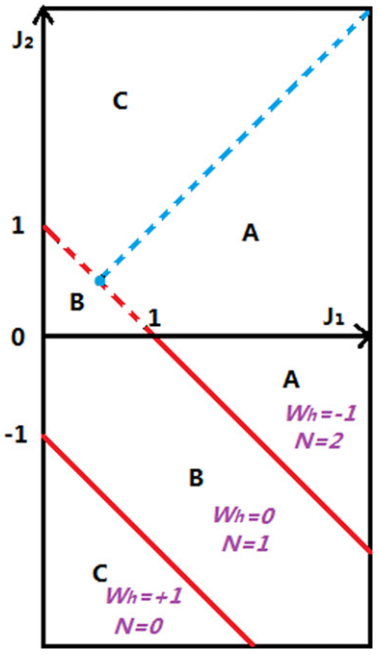

Fig. 2. Phase diagram of the Majorana snake chain Eq. (3). The lower panel of the diagrams ($J_2 < 0$) is the physical region, while the upper panel is a continuity to regions of $J_2 > 0$ (see Section 3).

Note that $J_- > |J_+|$ because of $J_1 > 0$ and $J_2 < 0$.

Since $J_- > 0$, the spectra vanishes for $k^* = 0$, $J_+ = -1$ and $k^* = \pm\pi$, $J_+ = 1$. As shown in the lower panel of Fig. 2, these two critical lines divide the J_1–J_2 parameter space into three gapped phases, namely, phase A: $J_2 > -J_1 + 1$; phase B: $-J_1 - 1 < J_2 < -J_1 + 1$; and phase C: $J_2 < -J_1 - 1$.

The transitions across the critical lines are of Ising type and described by the conformal field theory of a free massless fermion in $1+1$ dimensions with central charge equal to $1/2$. It was previously found that different phases can be characterized by string order parameters [8]. Indeed they are topologically distinct and can also be characterized by some kind of topological numbers. Note that the vector function $\mathbf{h}(k) = (h_1(k), h_2(k))$ defines a continuous mapping from the one-dimensional Brillouin zone to a 'h-loop' (which is an analogy to the h-surface defined for the two-dimensional Kitaev model [10]) in the (h_1, h_2) plane. The unit vector $\hat{\mathbf{h}}(k) = \mathbf{h}(k)/|\mathbf{h}(k)|$ is well defined in the three gapped phases and there exists an integral topological index

$$\mathcal{W}_h = \oint \frac{dk}{2\pi}\frac{\partial\theta_k}{\partial k}, \tag{6}$$

where the integral is taken over the Brillouin zone $k \in [-\pi, \pi]$, and the angle θ_k is defined as $(\cos\theta_k, \sin\theta_k) = \hat{\mathbf{h}}(k)$. The spectra collapses for $|\mathbf{h}(k)| = 0$, which is the origin of the h-space. So $\mathcal{W}$ counts the number of times the unit vector $\hat{\mathbf{h}}(k)$ wraps around the origin (see Fig. 3 for several examples).

Using $d\theta_k/dk = -\frac{d\cos\theta_k}{dk}/\sin\theta_k$, we find

$$\begin{aligned} \mathcal{W}_h &= -J_-\oint \frac{dk}{2\pi}\frac{J_+ + \cos k}{J_-^2\sin^2 k + (1 + J_+\cos k)^2} \\ &= -\frac{J_-}{2}\oint \frac{dz}{2\pi i}\frac{z^2 + 2zJ_+ + 1}{(J_1 z^2 + z + J_2)(J_2 z^2 + z + J_1)}, \end{aligned} \tag{7}$$

where we have used the change of variables $z = e^{ik}$ in the second line. The four poles of the integrand in the complex plane are $z_1 = (-1+X)/2J_1$, $z_2 = -(1+X)/2J_1$, $z_3 = 1/z_1$, and $z_4 = 1/z_2$, with $X \equiv \sqrt{1 - 4J_1J_2} > 1$, so that all the poles locate on the real axis.

Now we can study $\mathcal{W}_h$ in different phases.

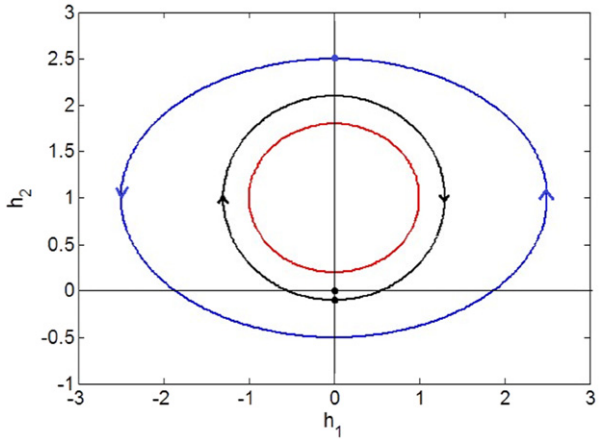

Fig. 3. The evolution of the 'h-loop' in different topological phases. The three different loops are selected from phase A, B and C respectively. Black: $(J_1, J_2) = (1.2, -0.1)$, red: $(J_1, J_2) = (0.9, -0.1)$; blue: $(J_1, J_2) = (0.5, -2.0)$. (For interpretation of the references to color in this figure legend, the reader is referred to the web version of this Letter.)

Phase A: $1 < X < 2J_1 - 1$, then $0 < z_1 < 1 - \frac{1}{J_1} < 1$, $-1 < z_2 < -\frac{1}{J_1} < 0$, the two poles z_1 and z_2 lie within the unit circle. Using the residue theorem, we get $\mathcal{W}_h = -1$;

Phase B: $|2J_1 - 1| < X < 2J_1 + 1$, then $-1 < z_1 < 1$, $-1 - \frac{1}{J_1} < z_2 < -1$, the two poles z_1 and z_4 lie within the unit circle and we get $\mathcal{W}_h = 0$;

Phase C: $X > 2J_1 + 1$, then $z_1 > 1 + \frac{1}{J_1} > 1$, $z_2 < -1 - \frac{1}{J_1} < -1$, the two poles z_3 and z_4 lie within the unit circle and we get $\mathcal{W}_h = +1$.

We see that the three different phases A, B and C are characterized by winding numbers $\mathcal{W}_h = -1, 0$ and $+1$, respectively. Thus, the winding number can be regarded as an order parameter of different phases and cannot change their values without gap closing.

It is easy to show that $\mathcal{W}_h$ is indeed related to the familiar winding number $\mathcal{W}_A$ of Anderson's pseudospin vector [11] defining the BdG Hamiltonian (in the momentum space of the Jordan–Wigner fermion representation) $H_{BdG}(k) = \mathbf{d}(k) \cdot \vec{\tau}$ via the relation

$$\mathcal{W}_h + \mathcal{W}_A = 1. \tag{8}$$

2.3. Majorana edge modes

In the preceding subsection, we identified three different phases of Eq. (3) and distinguished them by three different winding numbers. The winding number involves all momentum modes in the Brillouin zone, hence is a non-local quantity. In this subsection, we show that these phases can also be characterized by different types of Majorana edge modes.

In order to study the edge modes, we choose a snake chain of even $(2M)$ sites with open boundaries. Note that the snake chain is translationally invariant by two lattice spacings, so there are two possible ways to select an open chain with even sites, as shown in Fig. 4. In the case of Fig. 4(a), the system just reduces to Kitaev's p-wave superconducting model [1] holding none or one Majorana modes in different phases. Here we will study case (b) to establish a relation between the number (denoted by $\mathcal{N}$) of Majorana modes at one end of the chain and the corresponding winding numbers $\mathcal{W}_h$ in individual phases.

The open snake chain with $2M$ sites (Fig. 4(b)) is described by

$$H_2 = -i\left(\sum_{j=1}^{M-1} c_{2j}c_{2j+1} - J_2\sum_{j=1}^{M} c_{2j-1}c_{2j} + J_1\sum_{j=1}^{M-2} c_{2j}c_{2j+3}\right), \tag{9}$$

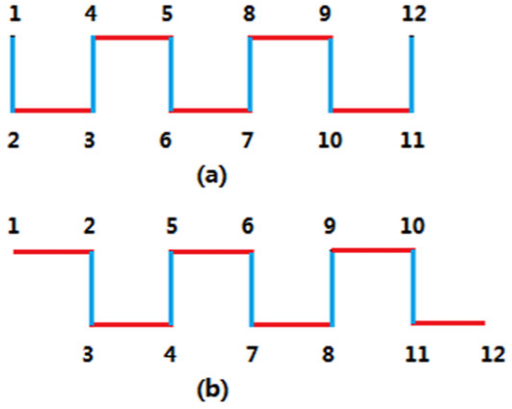

Fig. 4. Two choices of an even number snake chain with open boundaries.

whose phase diagram and bulk properties have been obtained in Section 2.2.

H_2 is of the standard quadratic form $H_2 = \frac{i}{4}C^T AC$, where $C = (c_1, c_2, \ldots, c_{2M})^T$ and A is a real antisymmetric matrix, and can be diagonalized by $W \in SO(2M)$ as follows [1],

$$H_2 = i\sum_{l=1}^{M} \epsilon_l b'_l b''_l, \qquad WC = \left(b'_1, b''_1, \ldots, b'_M, b''_M\right)^T. \tag{10}$$

Since $W \in SO(2N)$, we can choose W such that $W_{ij} = 0$ when the row and column index i and j are of different parities

$$b'_m = \sum_{l=1}^{M} W_{2m-1,2l-1}c_{2l-1}, \qquad b''_m = \sum_{l=1}^{M} W_{2m,2l}c_{2l}. \tag{11}$$

The recursive relations of $\{W_{2m-1,2l-1}\}$ and $\{W_{2m,2l}\}$ can be obtained from the Heisenberg equations of motion of operators $\{b'_m\}$ and $\{b''_m\}$,

$$i\dot{b}'_m = \left[b'_m, H_2\right] = 2i\epsilon_m b''_m, \qquad i\dot{b}''_m = \left[b''_m, H_2\right] = -2i\epsilon_m b'_m. \tag{12}$$

Combining Eq. (11) and Eq. (12), one obtains the following recursive relations $(l = 1, 2, \ldots, M)$

$$\begin{aligned} \epsilon_m W_{2m,2l} &= J_2 W_{2m-1,2l-1} + W_{2m-1,2l+1} + J_1 W_{2m-1,2l+3}, \\ \epsilon_m W_{2m-1,2l-1} &= J_1 W_{2m,2l-4} + W_{2m,2l-2} + J_2 W_{2m,2l}. \end{aligned} \tag{13}$$

Majorana zero modes correspond to $\epsilon_m = 0$. Here we emphasize the importance of boundary conditions: note that unphysical elements $W_{2m-1,2M+1}$ and $W_{2m-1,2M+3}$ ($W_{2m,-2}$ and $W_{2m,0}$) will emerge for $l = M-1$ and M ($l = 1$ and 2) in the first (second) equation and must be set zero. Thus, the required boundary conditions are

$$\begin{aligned} &W_{2m-1,2M-3} = W_{2m-1,2M-1} = 0, \\ &W_{2m,2} = W_{2m,4} = 0, \end{aligned} \tag{14}$$

for any physical solution.

From Eq. (13), the odd sector and even sector are decoupled and form two second order linear recurrence sequences. The characteristic equations of them read

$$J_1\lambda^2 + \lambda + J_2 = 0, \qquad J_2\eta^2 + \eta + J_1 = 0, \tag{15}$$

with solutions $\lambda_+ = z_1$, $\lambda_- = z_2$, $\eta_+ = z_3$, and $\eta_- = z_4$, where z_1, z_2, z_3 and z_4 are given in Section 2.2. Thus, we always have two distinct real roots for each equation and the corresponding general terms are given by

$$W_{2m-1,2l-1} = C_+\lambda_+^l + C_-\lambda_-^l,$$
$$W_{2m,2l} = C'_+\lambda_+^{-l} + C'_-\lambda_-^{-l}, \tag{16}$$

where the constants are determined by the boundary conditions. As discussed in Section 2.2, the absolute values of the four roots in different phases have different behaviors:

(i) In phase A, we have $|\lambda_\pm| < 1$, so there are two linearly independent solutions satisfying the boundary conditions Eq. (14), which correspond to two Majorana modes at each end of the chain;
(ii) In phase B, we have $|\lambda_+| > 1$, $|\lambda_-| < 1$. In order to satisfy Eq. (14), only the coefficients C_+ and C'_+ can be non-zero, corresponding to only one Majorana mode at each end;
(iii) In phase C, we have $|\lambda_\pm| > 1$. So there are no solution satisfying Eq. (14), i.e., there is no Majorana modes in this phase.

Now we obtain the relation between $\mathcal{N}$ and $\mathcal{W}_h$ in all of these phases:

$$\mathcal{N} + \mathcal{W}_h = 1. \tag{17}$$

Both $\mathcal{W}$ and $\mathcal{N}$ can be viewed as some kind of order parameter characterizing the corresponding topological phases.

It is believed that a spinless superconductor in one dimension is characterized by a Z_2 invariant [2–4]. However, in a recent work, Tewari and Sau [6] have demonstrated that such a Z_2 is incomplete and the topological invariant can indeed jump by two or other integers via a topological transition. This indicates that the topological index should be Z rather than Z_2, which is confirmed by the present study.

3. Broken time-reversal symmetry

The original model Eq. (1) protects time-reversal symmetry, which can be seen from the definition of time-reversal operation on spinless Jordan–Wigner fermions: $Ta_{j,\alpha}T^{-1} = a_{j,\alpha}$. It gives $Tc_jT^{-1} = (-1)^j c_j$ for the Majorana snake chain Eq. (3). Correspondingly, we have

$$T\Psi_k T^{-1} = -\sigma_3\Psi_{-k}. \tag{18}$$

Therefore, for a system with time-reversal symmetry, the Bloch matrix should satisfy

$$\sigma_3 H(k)\sigma_3 = H^*(-k). \tag{19}$$

Now we add a three-spin interaction [10]

$$H_t = \frac{J_4}{2}\sum_{j=1}^{N-1}\left(\sigma^x_{2j-1,1}\sigma^z_{2j,1}\sigma^y_{2j+1,1} + \sigma^y_{2j,1}\sigma^z_{2j+1,1}\sigma^x_{2j+2,1} + \sigma^y_{2j-1,2}\sigma^z_{2j,2}\sigma^x_{2j+1,2} + \sigma^x_{2j,2}\sigma^z_{2j+1,2}\sigma^y_{2j+2,2}\right) \tag{20}$$

to Eq. (1). In terms of Majorana operators this amounts to adding a fourth nearest-neighbor hoping to the snake chain representation Eq. (3)

$$H_t = -i\frac{J_4}{2}\sum_{j=1}^{2N-2}(c_{2j-1}c_{2j+3} - c_{2j}c_{2j+4}) = \sum_k \Psi_k^\dagger\left[h_3(k)\sigma_3\right]\Psi_k, \tag{21}$$

where $h_3(k) = J_4\sin 2k$. It is clearly seen that this term violets Eq. (19), so that breaks time-reversal symmetry.

We show that in the presence of time-reversal breaking term, phase A and phase C will be glued together to form a single phase.

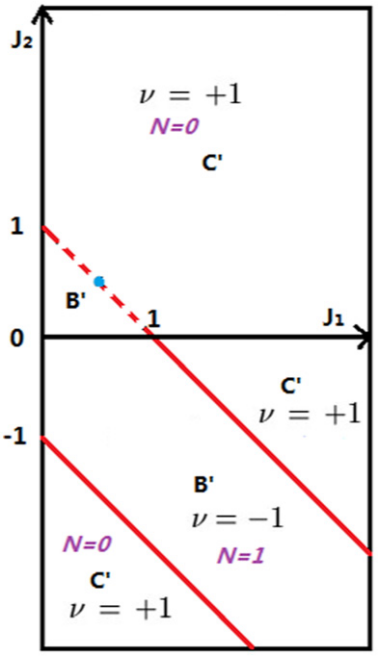

Fig. 5. Phase diagram of the Majorana snake chain with time-reversal symmetry being broken by the three-spin interaction. The lower panel of the diagrams ($J_2 < 0$) is the physical region, while the upper panel is continuity to regions of $J_2 > 0$.

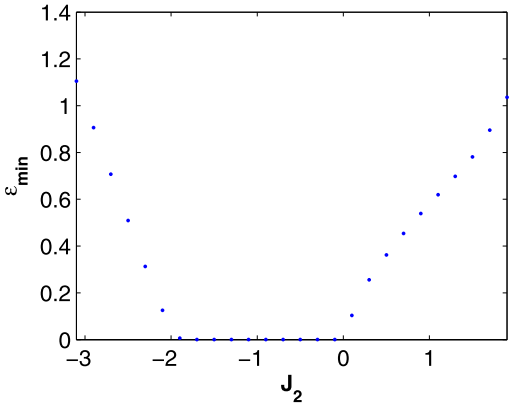

Fig. 6. $\epsilon_{\min}$ (ϵ_m with the minimal absolute value) as a function of J_2 ($J_1 = 1$, $J_4 = 1$, $M = 120$).

To the end, it is intuitive to make a continuity in the parameter space to allow for positive values of J_2. Of course, due to Lieb's theorem, the snake chain representation Eq. (3) is no longer a ground state Hamiltonian of the original spin model Eq. (1) in this case. But we can infer properties of Eq. (3) with $J_2 < 0$ from that of $J_2 > 0$.

Let us consider the case without H_t first. From Eq. (5), the spectra also vanishes at $k^* = \pm\pi$, $J_+ = 1$ in the extended parameter space, which is just a prolongation of the phase boundary between phase A and B in the region $J_2 < 0$ to $J_2 > 0$. Another critical line is $J_- = 0$ for $J_+ > 1$, where the spectra vanishes for $k^* = \pm\arccos(-\frac{1}{J_+})$. The transition across the latter belongs to the same universality class of the anisotropic transition of the XY chain and can be described by a conformal field theory with central charge equal to 1. The cross point of these two critical lines is special: the low energy dispersion vanishes quadratically at this point leading to the dynamical exponent $z = 2$. Indeed this is a multicritical point and the theory is no long conformal invariant. We see that the whole parameter space is divided into four regions by the three critical lines. By calculating the Majorana edge states or

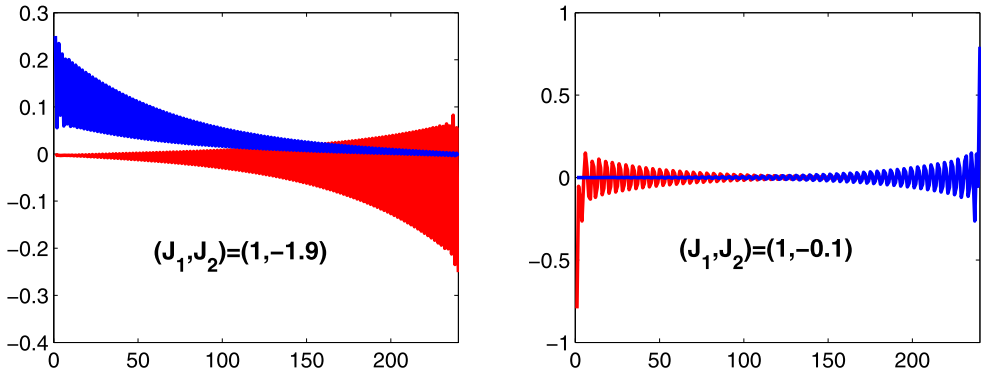

Fig. 7. There is one Majorana edge mode on each end of the chain for $(J_1, J_2) = (1, -1.9)$ (left) and $(1, -0.1)$ (right) ($J_4 = 1$, $M = 120$).

winding numbers similarly as before, we can easily show that they are just the extensions of phases A, B and C we have obtained for $J_2 < 0$, as shown in the upper panel of Fig. 2.

When H_t is present, the two branches of spectra become $\pm|\mathbf{h}(k)|$

$$\big|\mathbf{h}(k)\big| = \sqrt{J_-^2 \sin^2 k + (1 + J_+ \cos k)^2 + J_4^2 \sin^2 2k}. \tag{22}$$

It is interesting that H_t will open a gap along the critical line $J_- = 0$ and $J_+ > 1$ for $J_4 \neq 0$. This means that the original two phases A and C connect to each other to form a new phase C′. From symmetry considerations, we identify that the number of different phases reduces to only two now: phase B′ and C′, as shown in Fig. 5.

To confirm the above observation, let us consider Majorana modes at the ends in each phase. Let $b'_m = \sum_{l=1}^{M} W_{2m-1,2l-1} c_{2l-1} + W_{2m-1,2l} c_{2l}$ and $b''_m = \sum_{l=1}^{M} W_{2m,2l-1} c_{2l-1} + W_{2m,2l} c_{2l}$. Again, using the equations of motion, we obtain the following eigenvalue-eigenvector problem for the coefficients W_{ij}:

$$A^2 \mathbf{W}_i = -\epsilon_m^2 \mathbf{W}_i \quad (i = 1, 2) \tag{23}$$

where $\mathbf{W}_1 = (W_{2m-1,1}, W_{2m-1,2}, \ldots, W_{2m-1,2M})^T$, $\mathbf{W}_2 = (W_{2m,1}, W_{2m,2}, \ldots, W_{2m,2M})^T$ and $A_{2i-1,j} = J_1 \delta_{2i-4,j} + \delta_{2i-2,j} + J_2 \delta_{2i,j} - \frac{J_4}{2}(\delta_{2i-5,j} - \delta_{2i+3,j})$, $A_{2i,j} = -J_2 \delta_{2i-1,j} - \delta_{2i+1,j} - J_1 \delta_{2i+3,j} + \frac{J_4}{2}(\delta_{2i-4,j} - \delta_{2i+4,j})$, for $i = 1, 2, \ldots, M$ and $j = 1, 2, \ldots, 2M$.

In the presence of the time-reversal breaking term, the recursive relations cannot be solved analytically anymore due to the coupling between the odd and even sectors. Here we solve the recursive relation numerically for chains of finite sizes. Fig. 6 shows ϵ_m with the smallest absolute value (denoted by $\epsilon_{\min}$) as a function of $J_2 \in [-3.1, 1.9]$ along the line $J_1 = 1$, and we have chosen $M = 120$ and $J_4 = 1$. It is clearly seen that zero modes exist for $J_2 \in (-2, 0)$, which is just located within phase B′. There are no zero modes beyond this region, which corresponds to phase C′. Fig. 7 shows the amplitudes of the two orthogonal Majorana modes b'_m and b''_m at the two ends for $(J_1, J_2) = (1, -1.9)$ and $(1, -0.1)$, both of which are located in phase B′. Thus, there is no Majorana modes in phase C′, while one Majorana modes at each end in phase B′. In other words, the number of Majorana modes as an topological invariant collapses from Z to Z_2. In fact this Z_2 invariant is given by

$$\nu = \operatorname{sgn}\big[h_2(0) h_2(\pi)\big]. \tag{24}$$

$\nu = +1$ in phase B′ while $\nu = -1$ in phase C′. The collapsing of the topological invariants from Z to Z_2 also confirms the results of Ref. [6], since the time-reversal breaking term also breaks the chirality symmetry of the corresponding BdG Hamiltonian.

4. Conclusions

By studying an exactly soluble model, we show that the topological classification of the two-leg Kitaev ladder is characterized by an integer Z, rather than the commonly used Z_2 index. However, the Z index reduces to Z_2 in the presence of terms that break the time-reversal symmetry. These results are consistent with previous studies.

Acknowledgements

We thank Prof. G.M. Zhang for suggesting the original problem and enlightening discussions.

References

[1] A. Kitaev, Phys. Usp. 44 (Suppl.) (2001) 131.
[2] Z. Hasan, C.L. Kane, Rev. Mod. Phys. 82 (2010) 3045.
[3] X.L. Qi, S.C. Zhang, Rev. Mod. Phys. 83 (2011) 1057.
[4] J. Alicea, arXiv:1202.1293v1, 2012.
[5] Y.Z. Niu, S.B. Chung, C.H. Hsu, I. Mandal, S. Raghu, S. Chakravarty, Phys. Rev. B 85 (2012) 035110.
[6] S. Tewari, J.D. Sau, arXiv:1111.6592v2, 2012.
[7] A. Kitaev, Ann. Phys. (NY) 321 (2006) 2.
[8] X.Y. Feng, G.M. Zhang, T. Xiang, Phys. Rev. Lett. 98 (2007) 087204.
[9] E.H. Lieb, Phys. Rev. Lett. 73 (1994) 2158.
[10] D.H. Lee, G.M. Zhang, T. Xiang, Phys. Rev. Lett. 99 (2007) 196805.
[11] P.W. Anderson, Phys. Rev. B 110 (1958) 827.

ID	Title	Pages
1862220	Topological phases of the two-leg Kitaev ladder	5